ISSN 0010-9525, Cosmic Research, 2014, Vol. 52, No. 6, pp. 411–420. © Pleiades Publishing, Ltd., 2014.
Original Russian Text © N.A. Vlasova, V.V. Kalegaev, 2014, published in Kosmicheskie Issledovaniya, 2014, Vol. 52, No. 6, pp. 449–458.

Dynamics of Fluxes of Protons with Energies 30–80 keV during Geomagnetic Storms on January 21–22, 2005, and December 14–15, 2006, according to Data from Low-Orbit Satellites

N. A. Vlasova and V. V. Kalegaev

Skobeltsyn Institute of Nuclear Physics of Lomonosov Moscow State University

e-mail: nav19iv@gmail.com

Received January 23, 2013

Abstract—We present the results of a comparative analysis of the dynamics of three populations of fluxes of protons with energy 30–80 keV as measured by NOAA solar-synchronous satellites (*POES 15*, *16*, *17*) at low latitudes ($L < 2$) and at latitudes lower and higher than the boundary of isotropic precipitation during the geomagnetic storms on January 21–22, 2005 and December 14–15, 2006. Based on a complex analysis of experimental data on particle fluxes at low orbits and on measurements of solar wind parameters performed by the *ACE* spacecraft, we have studied the dynamical peculiarities of the fluxes of particles and of their longitudinal distributions depending on the conditions in the interplanetary medium. It is shown that an increase of trapped particle fluxes and the development of the main phase of the geomagnetic storm on January 21–22, 2005 are associated with the magnetosphere's response to a prolonged action of an extremely powerful coronal mass ejection at a northern orientation of the IMF. On December 14, 2006 an insufficient amplitude and duration of the pressure impulse did not result in development of a disturbance similar to January 21–22, 2005. The development of the main phase of this storm is related to a southward turn of the IMF, which has occurred only seven hours after the SSC.

DOI: 10.1134/S0010952514060082

INTRODUCTION

The spatial and temporal dynamics of particle fluxes in magnetospheric structures such as the plasma sheet of the magnetotail, ring current (RC), and the Earth's radiation belts [1] can be derived from data from measuring particle fluxes at low-orbit polar satellites. The dynamics of the spatial and temporal distributions of the particle fluxes is a result of changes in the magnetic and electric fields, and it can be used to describe electrodynamic processes in the near-Earth space environment [2, 3].

The most significant variations of particle fluxes occur in the Earth's magnetosphere during geomagnetic storms, whose development is intimately related with conditions on the Sun and with the situation of the interplanetary medium [4]. Under conditions of the southward orientation of the interplanetary magnetic field (IMF), the dawn–dusk electric field of the magnetotail accelerates plasma particles moving to the Earth. The intensification of magnetospheric convection and local accelerations of particles associated with substorm activity are basic processes that are responsible for the inflow of particles from the central plasma sheet of the magnetotail into the inner magnetosphere, to the region of capture of particles, and for the subsequent formation of the RC [3, 5].

The fluxes of particles measured by spacecraft reflect the magnetic field structure of the magnetosphere, and they can serve for diagnostics of the magnetosphere's current systems. On various segments of the orbit of a low-altitude satellite one can identify the region of isotropic precipitation, the region of a sharp drop of the fluxes of precipitating particles below the isotropization boundary (IB), and the near-equatorial region of trapped particles with large pitch-angles. These orbit segments are connected by magnetic field lines with regions in the near-Earth space possessing different physical properties. Changes in the magnetosphere associated either with external actions or with its inner dynamics lead to variations of the fluxes of particles of different populations and to variations of their boundaries.

The total energy of the precipitating protons in the dusk/night sector taken from data of the *POES 15* satellite was used for estimation of the rate of energy injection into the RC [1]. The assumption was substantiated that the flux value of precipitating protons detected by the satellite's instruments is an indicator allowing one to estimate amplitude of injection. It was shown that, the injection function being determined through fluxes of precipitating protons, the Burton equation allowed one to describe 70–80% of variation

of the corrected D_{st} index. This confirms the authors' idea that particles precipitating at high latitudes characterize the injection intensity rather than losses in the ring current. The dynamics of the RC during various phases of a geomagnetic storm was studied in [6] based on variations of low-latitude fluxes of protons of the storm time equatorial belt (STEB) according to measurement data of the *POES 15* and *POES 16* satellites. This phenomenon is caused by the interaction of energetic neutral atoms (ENA) moving to the Earth with ionospheric particles. These ENA are produced due to an exchange of the charges RC particles with neutral particles of the exosphere. It is shown that the longitude distribution of particles in this region is symmetrical on the storm recovery phase. The global pattern of precipitation of protons with energies 30–240 keV during a magnetic storm was obtained based on data of the *POES 15* and *POES 16* satellites [7]. The total energy of precipitating particles and the position of a maximum of proton precipitation are considered in this study. Based on measurements performed with MEPED instruments, it is shown that the region of precipitation of protons with energies 30–240 keV is displaced to lower latitudes with increasing geomagnetic activity. In this case, in accordance with the development of the storm ring current, the peak of precipitation is shifted to the equator and to the west.

Data provided by low-orbit polar satellites of the *POES* series were used to study the position and dynamics of the isotropization boundary (IB) above which isotropic fluxes of particles are observed [8, 9]. The authors of [9] associate the region of isotropic precipitation with strongly curved magnetic field lines, which lead to intense pitch-angle diffusion of particles and to their isotropic distribution. Using the statistical analysis of the data of two simultaneous measurements made by two low-orbit satellites of the *POES* series in [10], the latitude–longitude position of the isotropization boundary was studied as a function of interplanetary medium conditions and geomagnetic activity. In this paper it is demonstrated that with intensification of geomagnetic activity a motion of the IB to the equator is observed; the amplitude of motion of the IB dayside part is mainly determined by dynamics of solar wind pressure; motion in the evening sector is related to the dawn–dusk asymmetry of the magnetic field in the inner magnetosphere.

Ground-based and satellite measurements are indicative of a longitude asymmetry of the disturbed magnetic field during the main phase of a storm [11]. Asymmetry of the magnetospheric magnetic field reveals itself also in the longitude distribution of particle fluxes measured onboard low-orbit satellites [12]. Investigations of proton fluxes measured by the *Kosmos-900* satellite during geomagnetically quiet periods have shown that isotropic fluxes in the noon and morning sectors are observed on average at higher latitudes than in the night and evening sectors [13].

The goal of this paper is to study conditions in the magnetosphere during two geomagnetic storms (January 21–22, 2005 and December 14–15, 2006) different in strength and generated by unusual situations in the interplanetary space by making a comparative analysis of the dynamics and longitude distributions of particle fluxes. For the first time, distributions of fluxes of three populations of particles are studied simultaneously. They are detected at low ($L < 2$), moderate (below the IB), and high (above the IB) latitudes, and their energies belong to the RC particles energy range. Measurements are made simultaneously by three satellites: *POES 15, POES 16*, and *POES 17*. Special attention will be paid to dynamics of the fluxes of charged particles and to a possible mechanism of formation of the ring current during the storm on January 21–22, 2005 whose main phase occurred under conditions of a northward IMF.

EXPERIMENTAL DATA

The experimental data on which the work is based are obtained by three low-orbit solar-synchronous satellites: *POES 15*, *POES 16*, and *POES 17* [http://satdat.ngdc.noaa.gov/sem/poes/data/avg/txt/]. The *POES* satellites are polar satellites with circular orbits of a height of ~800 km and a period of revolution ~100 min. The satellite orbit is such that for a limited time period its ascending and descending legs are permanently located approximately at the same local times. For example, in January 2005, *POES 15*, crossing the geomagnetic equator, was located in the region ~06 and ~18 MLT; *POES 16* was in the region ~02 and ~14 MLT; and *POES 17* in the region ~10 and ~22 MLT. "Almost simultaneous" (as a rule, made within half an hour) measurements in each hemisphere by three satellites for six MLT values give a possibility to reconstruct longitude distributions of particle fluxes.

Measurements of the fluxes of energetic protons on the *POES* satellites were made by the MEPED instrumentation [14]. Two mutually perpendicular detectors register particles in the radial direction (the 0-detector along the Earth's radius) and along the satellite orbit (the 90-detector). At high latitudes the 0-detector and 90-detector measure precipitating particles and trapped (quasi-trapped) particles, respectively, while on the equator the situation is opposite. It should be noted that in the context of IGRF11 model of geomagnetic field 0- and 90-detectors register the fluxes of particles with identical pitch-angles at magnetic latitudes ~22°–36°, which corresponds to an L parameter value of less than 2.

Let us consider fluxes of protons with energy 30–80 keV measured by 0- and 90-detectors during satellite passages over the Earth's northern hemisphere. A typical time profile of the proton fluxes measured by the *POES 15* satellite during the main phase of the magnetic storm on January 22, 2005 is presented in

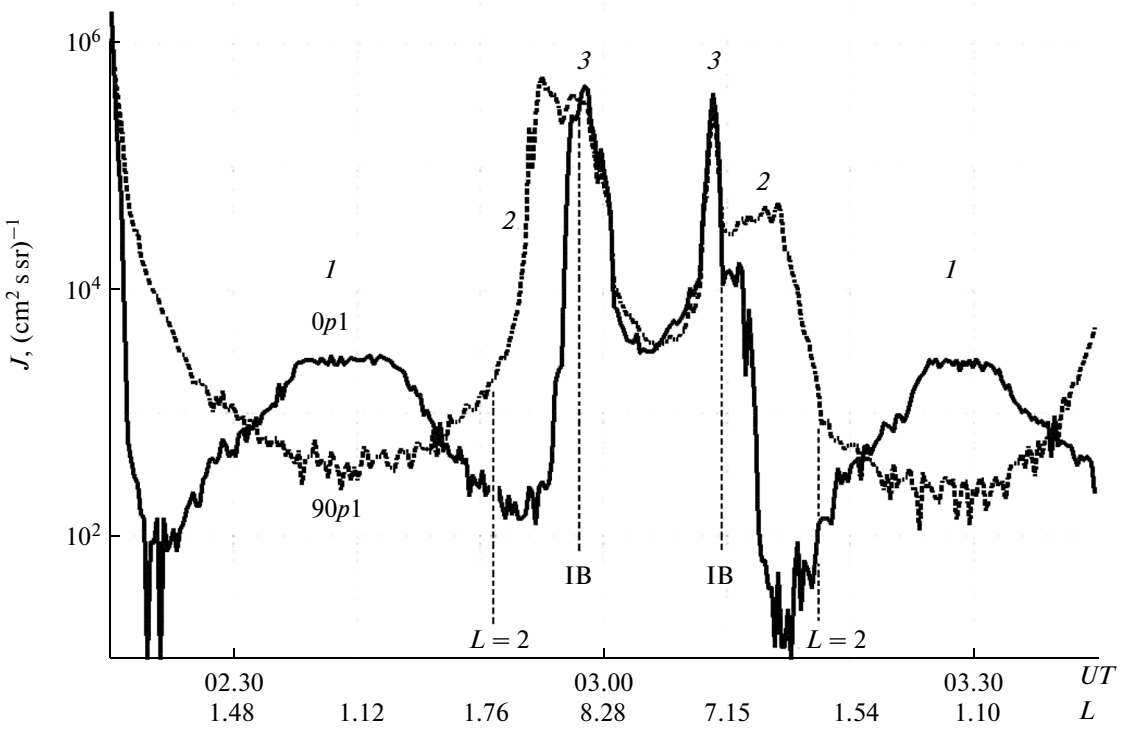

Fig. 1. Time profiles of the fluxes of protons with energies 30–80 keV (the data of 0-detector and 90-detector are represented by solid and dashed curves, respectively). Vertical dashed lines correspond to positions of isotropization boundary and $L = 2$. Numerals *1*, *2*, and *3* designate the regions of satellite orbits where dynamics of particle fluxes was investigated (see text).

Fig. 1. The particle fluxes were measured by 0- and 90-detectors (solid and dashed lines, respectively). The fluxes of particles recorded by 0- and 90-detectors are nearly identical at high latitudes; in the region of adiabatic motion of particles at lower latitudes the fluxes of 90-detector prevail. The IB is a place where one observes going out from the region of relative equality of particles fluxes recorded by 0- and 90-detectors, i.e., from the region with isotropic pitch-angle distribution of the particle fluxes [9].

Dynamics of the fluxes of energetic protons was studied in three characteristic regions in orbits of each of three *POES* satellites (Fig. 1).

Region 1. Near-equatorial region below $L \sim 2$, where maximum fluxes of trapped protons were determined using the data of 0-detector. Passages near the South-Atlantic Anomaly (SAA) region were not considered, which substantially reduced the number of experimental points and led to gaps in the longitude profile of fluxes.

Region 2. At middle latitudes, where the total flux of protons was calculated according to 90-detector data in the region from $L \sim 2$ (where the particle flux approaches background values) up to IB, where proton fluxes measured by 0- and 90-detectors become close ($L \sim 2$ and IB are shown in Fig. 1 by dashed lines).

Region 3. The high-latitude region above the IB, where maximum intensities of fluxes of precipitating particles were determined using 0-detector data.

The impact of radiation on the detectors has already led to their degradation after two years of operation in open space [15]. Analyzing the fluxes of trapped particles measured by satellites on the recovery phases of geomagnetic storms on January 21–22, 2005 and December 14–15, 2006, it has been shown that their intensity differs by a factor of 2, and they need an additional calibration. Therefore, for all data of *POES 15* and *POES 16* satellites used below normalizing coefficients were introduced for matching with the *POES 17* satellite data (*POES 17* was selected as a most advanced satellite). The normalizing coefficients for the storm of January 21–22, 2005 are as follows: $J(POES\ 17)/J(POES\ 15) = 1.94$ and $J(POES\ 17)/J(POES\ 16) = 1.34$; while for the storm on December 14–15, 2006 we have $J(POES\ 17)/J(POES\ 15) = 2.12$ and $J(POES\ 17)/J(POES\ 16) = 1.4$. In what follows normalized values will be used for the fluxes.

It should be noted that due to prolonged stay in open space the boundaries of energy intervals are also variable [15]. The normalizing coefficients introduced above implicitly take this effect into account too: calculated fluxes correspond to common energy channels for all satellites. At the same time, real channel boundaries remain undetermined. According to estimation in [15] the lower boundary for the 30–80 keV channel equals about 45 keV for *POES 17*. Below, we will continue using nominal designations for the channels.

In order to investigate external actions upon the conditions of the magnetosphere, the data on parameters of the interplanetary medium provided by the *ACE* spacecraft were used [www.ssg.sr.unh.edu/mag/acr; www.sec.noaa,gov/ftpdir/lists/ace]. This spacecraft is placed to a libration point (at a distance of about 1.5 million km from the Earth to the Sun). As characteristics of the Earth's magnetosphere conditions the following geomagnetic indices were used: the *Dst* variation, *ASY-H*, *SYM-H*, and *AL*-indices (World Data Center C2 for Geomagnetism, Kyoto [http://wdc.kugi.kyoto-u.ac.jp/]).

RESULTS AND DISCUSSION

The geomagnetic storms on January 21–22, 2005 and December 14–15, 2006 have many common features; in particular, their time profiles of *Dst* variation have similar shapes (a flat drawn-out minimum or flat phase). However, in many respects they are different (Fig. 2).

The geomagnetic storm of January 21–22, 2005 was produced by the arrival of the front of a powerful shock wave at a short southward IMF orientation, the main phases of the storm having occurred under conditions of positive B_z in the solar wind. The storm on December 14–15, 2006 began after a compression of the magnetosphere by a cloud of accelerated dense plasma, but the main phase began approximately in 7 h, when the IMF B_z had become negative. There are two well-pronounced positive variations of the magnetic field in *Dst* profile, they are associated with compression of the magnetosphere. One can see that, unlike the January 21–22, 2005 event, no magnetic storm development occurred after the first SSC under the northward IMF, but southward rotation of the IMF at 22 UT resulted in efficient energy transfer from solar wind into the magnetosphere and in the development of a strong geomagnetic disturbance.

As is noted above, one can discern three populations of particles on the time profile of proton fluxes measured during a passage of the *POES* satellites from the equator to the polar cap (see Fig. 1): particles trapped in equatorial region 1; particles of region 2 below IB at middle latitudes; and particles precipitating above the IB in region 3. Fluxes of particles in the Earth's magnetosphere are controlled by the magnetospheric magnetic field, while their variations reproduce the dynamics of magnetospheric currents in response to external action of the solar wind. Time profiles of the fluxes of all three populations of particles obtained according the procedure described in the previous section are presented in Fig. 3 together with time profiles of geomagnetic activity indices for January 21–21, 2005 and December 14–15, 2006. When representing the fluxes a separate designation is used for every MLT (see legend in Fig. 3). For the sake of simplicity of the plots, the second and lower panels show only data obtained in the evening hemisphere. For better visualization, the experimental points obtained during the night hours are connected by lines.

In Fig. 3a one can see the dynamics of the fluxes of trapped protons (particles of region 1). Under quiet conditions before the onset of geomagnetic storms the longitude asymmetry of fluxes of trapped protons is insignificant. One can see increased fluxes with a maximum in the storm's main phase (immediately after *SSC* in January 2005 and in the period of minimum values of *SYM-H* in December 2006) and decreased fluxes in the phase of recovery.

A sharp increase of fluxes on January 21, 2005 begins not in the main phase, but immediately after arrival of the shock wave front accompanied by two short southward rotations of the IMF. The fluxes of trapped particles reproduce specific features of the ring current dynamics in the course of magnetic storms development. The "geoeffective" IMF direction (Fig. 2) was observed only for two hours, being accompanied by extreme compression of the magnetosphere due to a strong impact of the solar wind. It has resulted in intensified fluxes of trapped particles, which, according to [6], is indicative of a powerful ring current developed during the magnetic storm in January 2005. One can see that the longitude distribution of trapped particle is always symmetrical, except for initial and main phases, which coincide in time with a period of asymmetry of the magnetic field, determined using variations of the *ASY-H* index (Fig. 3g). The maximum fluxes are detected in the pre-midnight hours. However, in the period of southward IMF direction the fluxes in the post-midnight sector also increase. The analysis made indicate to a close link between the fluxes of trapped particles and variation of storm's magnetospheric magnetic field (mainly associated with the development of symmetric and asymmetric ring current) that forms the profiles of *ASY-H* and *SYM-H*.

Figure 3b presents the time profiles of the particle flux in region 2 (predominantly RC particles with small pitch-angles that are close to the loss cone). The dynamics of the particle fluxes in region 2 and that of trapped near-equatorial particles of region 1 are similar. This is not surprising, since the trapped particles of region 1 demonstrate peculiarities of ring current particles, which partly are located at the same L-shells as particles of region 2 [6]. At latitudes below IB (see Fig. 1) the particle flux measured by 0-detector can be reduced by 5 orders of magnitude, while measurements by 90-detector demonstrate a gradual drop without a well-distinguished boundary, frequently forming a maximum. The particles populating this region are trapped by the geomagnetic field, and they participate in the formation of the ring current. At the same time, these particles have equatorial pitch angles close to the loss cone, representing only a small and unstable part of it. Wave processes in the magnetosphere represent one mechanism of ring current decay. They can result in a pitch-angle scattering of particles

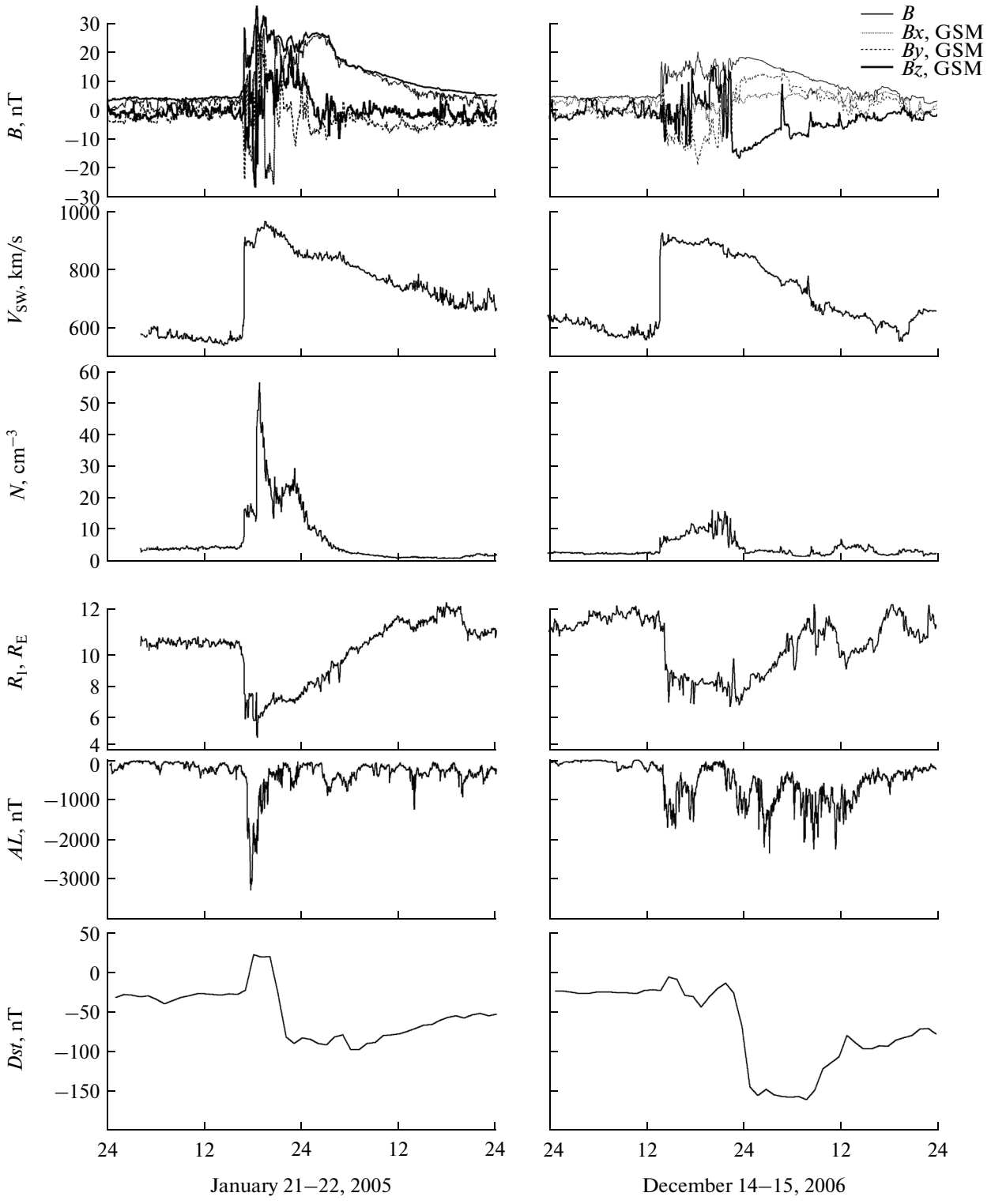

Fig. 2. Time profiles of magnitude (B) and components (B_{xyz}) of the IMF, velocity (V_{SW}) and density (N) of the solar wind, distance (calculated according to model of [16]) to subsolar point of the magnetopause, and indices of geomagnetic activity (*AL* and *Dst*).

due to their resonance interaction with waves [17, 18]. In this case one can observe the fluxes of precipitating particles below the IB [19, 20]. Forced changes in the magnetosphere occurring under the action of the solar wind also lead to substantial variations of particle fluxes in region 2. Non-synchronous variations of the

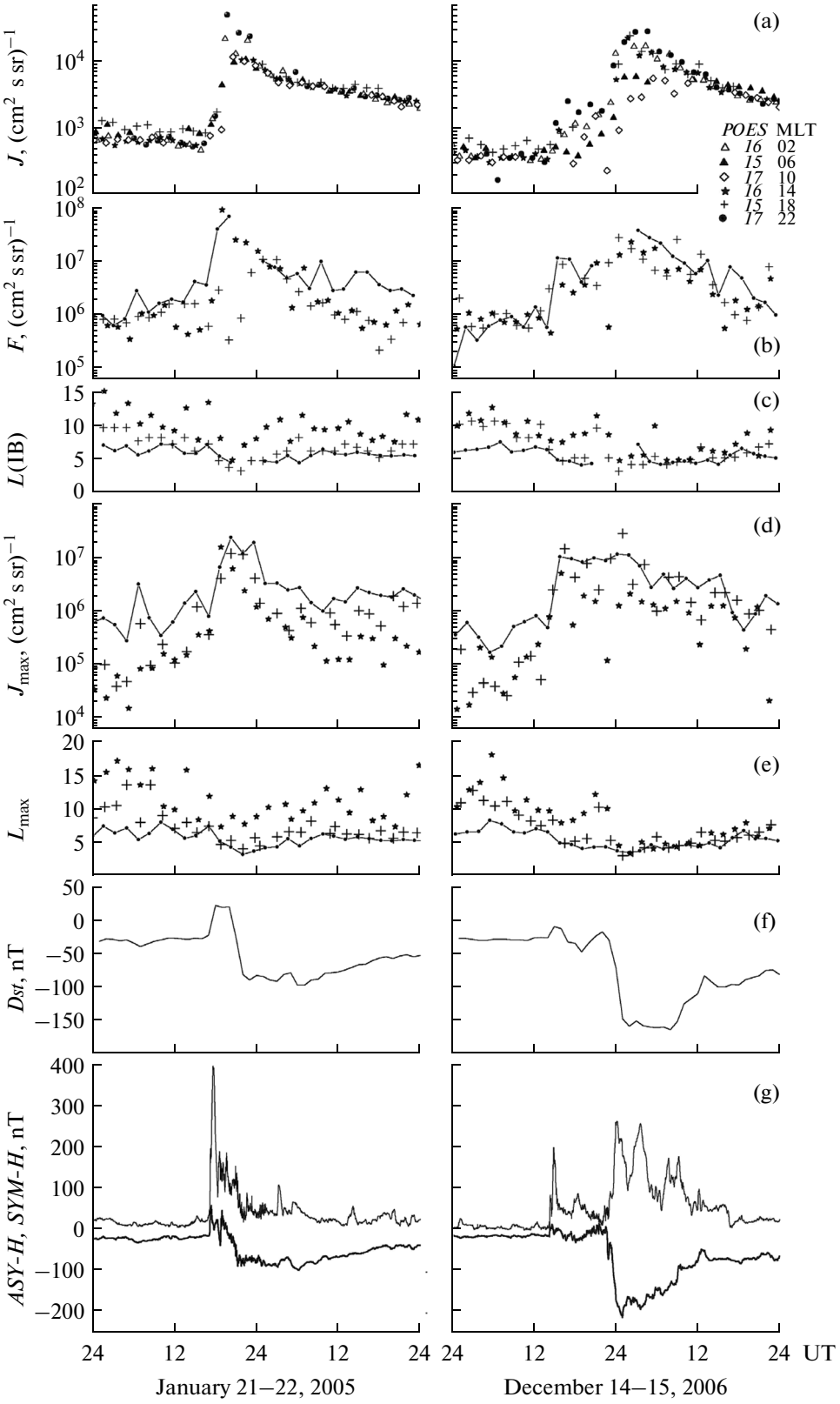

Fig. 3. Time profiles of maximum fluxes of trapped protons (a), total proton fluxes of region 2 (b), L-positions of the isotropization boundary (c), maximum fluxes of trapped protons (d), their L-positions (e), amplitude of Dst variation (f), and indices *ASY-H* (upper curve) and *SYM-H* (lower curve) (g).

fluxes at different MLT are indicative of local processes acting upon the population of these particles: unlike trapped particles, the fluxes in region 2 are distributed asymmetrically throughout the entire storm both in January 2005 and December 2006.

On January 21–22, 2005 the maximum fluxes were detected during the SSC, being rapidly diminished after that. This probably can be associated with the displacement of the plasma sheet to the Earth during the storm's main phase and with the expansion of the isotropic region, which in turn resulted in the reduced dimensions of the zone of quasi-trapping. Because of this, it becomes difficult to identify the IB in the night sector. Another factor complicating the IB identification is the above-mentioned development of wave processes in the magnetosphere, which results in isotropization of the fluxes of trapped particles [8, 19]. The fact that data in the pre-midnight sector are unavailable after the *SSC* maximum is related to the impossibility of determining the IB position due to the overlapping of these two effects.

We assume that the IB is a high-latitude boundary of region 2. It is determined according to the procedure of [9] as a point below which the particle fluxes measured by the *POES* 90-detectors are essentially predominant. Dynamics of the IB position over L-parameter is presented in Fig. 3c. In order to get IB dependence on invariant latitude ϕ_{inv} one can take advantage of the relationship: $L = 1/\cos^2(\phi_{inv})$. The position of the isotropization boundary is asymmetric in space: the night sector is considerably lower in latitude than the dayside sector. With increasing geomagnetic activity the IB is displaced to the equator at all longitudes, in accordance with the results of [10]. The largest changes take place in the dayside sector, while the night segment of the boundary varies insignificantly. On the main phase of the storms the IB has most symmetrical position.

At higher latitudes the *POES* satellites detect isotropic particle fluxes of region 3, which are projected onto bases of magnetic field lines connecting the ionosphere with the plasma sheet. Figure 3d presents the time profiles of the flux of precipitating particles. It is shown in paper [1] that sharp increases of particle fluxes above the IB characterize the process of injection from the plasma sheet (where particles are accelerated by electric and magnetic fields, and move adiabatically) into the inner magnetosphere. The dynamics of the longitudinal distribution of the fluxes of precipitating particles is presented in Fig. 4, symbols at each curve representing the UT moment. Since satellites do not pass through places with maximum fluxes of precipitating particles simultaneously, and flux variations during storms are relatively fast, longitude distributions of maximum fluxes for given UT values were obtained from time profiles by linear interpolation. Thus the obtained dependencies are divided in two groups: the upper panel presents increasing fluxes (up to maximum values) in the storm maximum, while the lower panel shows decreasing fluxes (down from the same maximum values) on the recovery phase. To complete (the cyclic character of) the longitude distribution curve the MLT scale expanded by 12 h, and the flux value for early morning hours is repeated twice.

In spite of large flux variations, especially strong on December 14–15, 2006, one can discern a general tendency for all curves: the fluxes increase from morning hours to midnight (Fig. 4). This is indicative of a permanent asymmetry of the longitudinal distribution of maximum fluxes of precipitating protons and is due to proton drift from the night sector through evening and day to morning. A sharp increase of fluxes is observed at all longitudes during interactions of CMEs with the magnetosphere. Before this the minimum and maximum fluxes are detected in morning and pre-midnight hours, respectively. At the moment of SSC the fluxes of particles in the pre-midnight sector demonstrate the largest increase. These fluxes dominate during the total period of magnetosphere compression: during the storm of January 2005 this period is rather long, and in December 2006 it is shorter. Increased fluxes in the post-midnight sector are accompanied by strong variations of the *AL*-index. Presumably, they are associated with development of the injection mechanisms that accompany substorm activity. After the main phase the pre-storm profile of flux distributions is reshaped, and the flux value is regenerated with the beginning of the recovery phase.

The L-parameter dynamics of the maximum of precipitating particles presented in Fig. 3e is similar to the dynamics of the IB position. Minimum values of L for both positions are reached during the storm main phase, at the *Dst* minimum. In [21] the RC structure is calculated, and the following relationship (derived previously in an empirical way) between the position L_{max} of maximum of the belt of relativistic electrons injected during magnetic storms and the magnetic storm amplitude is substantiated: $|Dst|_{max} = 2.75 \times 10^4 L_{max}^{-4}$ [22]. In [21] it has been also shown that the L_{max} position corresponds to the region of maximum relative attenuation of the field at the largest $|Dst|_{max}$ value, and, possibly, it characterizes the region of maximum pressure of RC plasma. According to this relationship, $L_{max} \sim 4.02$ for the geomagnetic storm of January 21–22, 2005 with $|Dst|_{max} = 97$ nT, and $L_{max} \sim 3.48$ for the geomagnetic storm on December 14–15, 2006 with $|Dst|_{max} = 157$ nT.

According to the *POES* satellite data, during the maximums of both considered storms the IB and maximums of precipitating protons are also located at close L-shells: about 3.5 near midnight. In should be noted in this case that reduced L values of the IB position during the storm maximum do not reflect equally significant variations of outer boundaries of the ring current in its equatorial part. This is due to distortions of the magnetic field in the inner magnetosphere because of storm development of magnetospheric currents (ring and magnetotail currents). Of course, the RC position

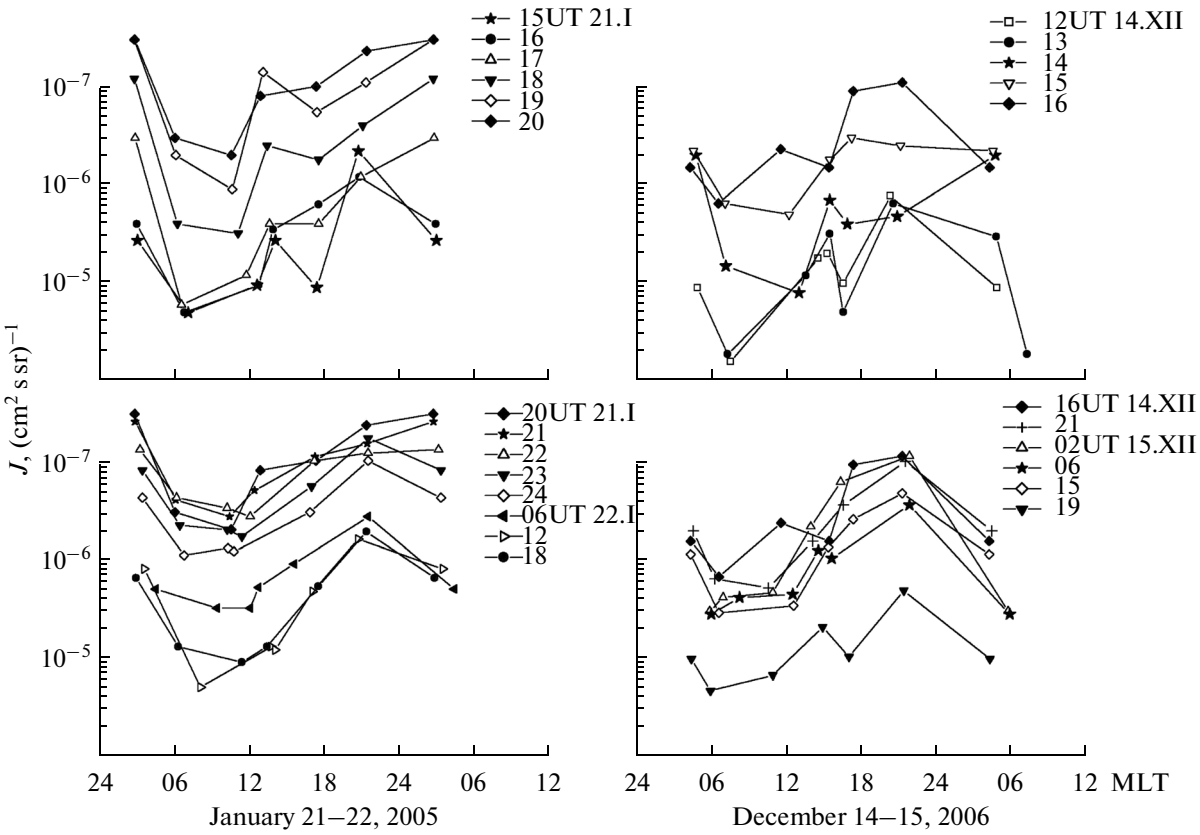

Fig. 4. Longitude distributions of interpolated values of the maximum fluxes of precipitating protons.

does not determine positions of the IB and maximums of precipitating protons, as the above formula, but similar dynamics during storms allows one to make conclusions about the magnetosphere state and to compare the two storms under study.

One can see in Figs. 3a, 3b, and 3d that on January 21–22, 2005 the maximum fluxes of all populations are comparable with those for December 14–15, 2006, or even exceed them, though $|Dst|_{max}(2005) = 97$ nT is almost half as much as $|Dst|_{max}(2006) = 157$ nT (Fig. 3f). The discrepancy between particle fluxes and magnetic field variations is, apparently, associated with different mechanisms of development of the magnetic storms under consideration. Approximately identical L positions of isotropization boundaries and maximums of precipitating particles at *Dst* minimums of both the storms (Figs. 3c and 3e) (in spite of their different strength) can be indicative of an identical "depth of flow" of the RC inside the magnetosphere. On December 14–15, 2006 such a position of the ring current corresponds to the storm strength (which is confirmed by agreement with estimates made using the above formula from paper [22]), while on January 21–22, 2005 the ring current power and position do not correspond to the magnetic field variations observed on the Earth's surface. In the absence of geoeffective IMF on the storm main phase one could expect the existence of specific processes of ring current formation. In our opinion, this could be reached on January 21–22, 2005 owing to an extremely powerful compression of the magnetosphere during the SSC, which ensured penetration of plasma inside the magnetosphere and its additional energization. Deep location of the RC inside the magnetosphere, increasing the magnetic effect of particle fluxes, could form a "flat" phase of the storm up to ~06 UT on January 22, 2005, until the magnetosphere spatial dimensions were recovered up to the pre-storm values (Fig. 2).

The extreme compression of the magnetosphere has an effect on particle fluxes in the magnetosphere (especially that of January 2005, Fig. 2), and it can become one of the most important sources for ring current formation. One can suppose that a fast compression of the magnetosphere at the initial moment of *SSC* had resulted in non-adiabatic displacement of particles to lower L-shells with violation of the third adiabatic invariant, accompanied by their energization. The subsequent slow recovery of dimensions of the magnetosphere (for approximately 10 h, which exceeds the drift motion period for bulk population of ring current particles with energies of 30–80 keV) occurred adiabatically, without particle return to previous orbits. Such a mechanism of RC formation is

similar to the mechanism of radial transfer of particles of the radiation belts by sudden impulses [23], differing only in the time scale of the process.

In January 2005 we see sharp increases of the fluxes in all populations of particles at the moment of prolonged *SSC*. Attention should be paid to the fact that flux values both in region 2 and of precipitating particles immediately after SSC in dayside sector exceeded night sector fluxes (see Figs. 3b and 3d). From ~19 UT, in spite of the IMF orientation having become northward, *Dst* was decreasing, the fluxes of trapped particles were growing, while the ring current continued to develop. The recovery phase occurred when density of solar wind plasma went back to pre-storm values approximately at ~06 UT on January 22, 2005.

A pressure impulse at ~14 UT on December 14, 2006 also resulted in a positive variation of *Dst* (Fig. 2). However, under the northward IMF there was no development of a disturbance similar to that in the storm on January 21–22, 2005, probably, because the solar wind impact during the *SSC* was not sufficiently strong. The storm continued to develop only for 7 hours, when the IMF B_z values became negative, which represented the main factor determining geomagnetic conditions on December 14–15, 2006. It is interesting to note that southward rotation of the IMF on the background of stably increasing plasma pressure values caused an additional displacement of the magnetopause to the Earth, which revealed itself as a noticeable positive variation of *Dst* (recurrent *SSC*) a day before the main phase.

At the southward IMF orientation under conditions of auroral activity during the main and long "flat" phases of the storm on December 14–15, 2006, there existed a powerful flux of energy from the interplanetary medium into the magnetosphere [24]. It ensured a long-term injection of plasma from the magnetotail to the ring current region. Numerous manifestations of auroral activity during the main and flat (unlike 2005 storm, see *AL* variations in Fig. 2) resulted, possibly, in flatter profiles of particle fluxes in region 2 and of precipitating particles (see Figs. 3b and 3d). Also, from the beginning of the main phase of the storm on December 14–15, 2006, the boundaries of isotropic precipitation and positions of maximums of precipitating particles became more symmetric in longitude (see Figs. 3c and 3e), which can indicate to an important role played by substorm mechanisms in development of this disturbance. When the IMF B_z component returned to background values, the rate of particle influx to the inner magnetosphere decreased, and this led to the beginning of ring current decay on the recovery phase.

CONCLUSIONS

Using the data of low-orbit satellites *POES 15*, *POES 16*, and *POES 17* dynamics of particle fluxes and their longitude distributions have been studied for magnetic storms on January 21–22, 2005 and December 14–15, 2006. Three different populations of particles were investigated: at low latitudes ($L < 2$), and above and below the boundary of isotropic precipitation. Comparative analysis of the particle fluxes, solar wind parameters, and geomagnetic indices has shown that the dynamics of particle fluxes reflects variations of the solar wind. Specific features of dynamics of the particle fluxes under study can serve as indicators of the magnetosphere conditions.

It is shown that variations of the particle fluxes of all populations take place in all longitudes at the moment of interaction of accelerated solar wind with the magnetosphere. The maximum fluxes of precipitating particles are located in the pre-midnight sector during quiet periods and at all storm phases excluding SSC period, when fluxes at early morning hours dominate. The longitude distribution of the fluxes of trapped particles is symmetrical during a magnetic storm; asymmetry is observed only during *SSC* and the storm main phase.

In spite of the different strengths of the storms on January 21–22, 2005 and December 14–15, 2006 ($|Dst|_{max}(2005) = 97$ nT and $|Dst|_{max}(2006) = 157$ nT), approximately equal fluxes of the three populations were observed at *Dst* minimums of both the storms, as well as close L-positions of both isotropization boundary and maximums of precipitating particles. If, according to [6], the fluxes of trapped particles measured onboard low-orbit satellites can serve as a proxy for the ring current, similarity of their flux values and dynamics of isotropization boundary testify identical characteristics of the ring current and its position inside the magnetosphere for both the storms. A comparison of the magnetic effects of the storms shows that there is no common relationship between measured parameters of particle fluxes and *Dst* variation value in this case. One can suppose that the ring current was a dominant source of the magnetic field variation in the January 2005 storm, and the extremely strong compression of the magnetosphere during SSC was a source of so powerful development of the ring current. At the same time on December 14–15, 2006 the ring current development was associated with traditional mechanisms of injection controlled by the solar wind electric field.

ACKNOWLEDGMENTS

The authors thank I.I. Alexeyev, L.L. Lazutin, and G.P. Lyubimov for useful discussions and N.N. Pavlov for used mathematical apparatus. They also express their gratitude to reviewers whose remarks helped to make the text shorter, more readable and clear, to eliminate uncertainties and to improve definitions. The data on the solar wind and geomagnetic indices were taken in the Goddard Space Flight Center of NASA (Omniweb) and in the World Data Center C2 for Geomagnetism, Kyoto. The experimental data of *NOAA/POES* measurements were obtained in the

NOAA's National Geophysical Data Center. The work is supported by the RF Ministry of Education and Science, contract no. 14.604.21.0049.

REFERENCES

1. Søraas, F., Aarsnes, K., Oksavik, K., and Evans, D.S., Ring current intensity estimated from low-altitude proton observations, *J. Geophys. Res.*, 2002, vol. 107, no. A7, pp. 1149–1859. doi: 10.1029/2001JA000123
2. Alfven, H. and Fälthammar, C.-G., *Cosmical Electrodynamics, Fundamental Principles*, New York: Oxford Univ. Press, 1963.
3. Tverskoy, B.A., Electric fields in the magnetosphere and the origin of trapped radiation, in *Solar-Terrestrial Physics*, Dyer, E.R., Ed., Dordrecht, Holland: D. Reidel, 1972, pp. 297–317.
4. Gonzalez, W.D., Joselyn, J.A., Kamide, Y., et al., What is a geomagnetic storm?, *J. Geophys. Res.*, 1994, vol. 99, no. A4, pp. 5771–5792.
5. Kozyra, J.U. and Liemohn, M.W., Ring current energy input and decay, *Space Sci. Rev.*, 2003, vol. 109, nos. 1–4, pp. 105–131. doi: 10.1023/B:SPAC.0000007516.10433.ad
6. Søraas, F., Oksavik, K., Aarsnes, K., et al., Storm time equatorial belt—an "image" of RC behavior, *Geophys. Res. Lett.*, 2003, vol. 30, no. 2, pp. 1052–1055. doi: 10.1029/2002GL015636
7. Fang, X., Liemohn, M.W., Kozyra, J.U., et al., Global 30–240 keV proton precipitation in the 17–18 April 2002 geomagnetic storms: 1. Patterns, *J. Geophys. Res.*, 2007, vol. 112, A05301. doi: 10.1029/2006JA011867
8. Gvozdevsky, B.B., Sergeev, V.A., and Mursula, K., Long lasting proton precipitation in the inner magnetosphere after substorms, *J. Geophys. Res.*, 1997, vol. 102, no. A11, pp. 24333–24338.
9. Sergeev, V., Malkov, M., and Mursula, K., Testing the isotropic boundary algorithm method to evaluate the magnetic field configuration in the tail, *J. Geophys. Res.*, 1993, vol. 98, no. A5, pp. 7609–7620. doi: 10.1029/92JA02587
10. Lvova, E.A., Sergeev, V.A., and Bagautdinova, G.R., Statistical study of the proton isotropy boundary, *Ann. Geophys.*, 2005, vol. 23, pp. 1311–1316.
11. Akasofu, S.-I. and Chapman, S., On the asymmetric development of magnetic storm fields in low and middle latitudes, *Planet. Space Sci.*, 1964, vol. 12, pp. 607–626.
12. Morozova, T.I., Panasyuk, M.I., Sosnovets, E.N., et al., Dynamics of dusk–dawn asymmetry of the ring current during the magnetic storm on December 1–2, 1977 as derived from data of *Kosmos-900* satellite, *Geomagn. Aeron.*, 1982, vol. 22, no. 4, p. 699.
13. Panasyuk, M.I., Reizman, S.Ya., and Sosnovets, E.N., Spatial distribution of protons at high and low altitudes in radiation belts: Comparison of theory and experiment, *Cosmic Research*, 1985, vol. 23, no. 6, p. 714.
14. Evans, D.S. and Greer, M.S., *Polar Orbiting Environmental Satellite Space Environment Monitor, 2. Instrument Descriptions and Archive Data Documentation, NOAA Tech. Memo. OAR SEC-93*, Boulder, Colo.: NOAA, 2000.
15. Asikainen, T., Mursula, K., and Maliniemi, V., Correction of detector noise and recalibration of NOAA/MEPED energetic proton fluxes, *J. Geophys. Res.*, 2012, vol. 117, A09204. doi: 10.1029/2012JA017593
16. Shue, J.-H., Song, P., Russell, C.T., et al., Magnetopause location under extreme solar wind conditions, *J. Geophys. Res.*, 1998, vol. 103, no. A8, pp. 17691–17700. doi: 10.1029/98JA01103
17. Kennel, C.F. and Petchek, H.E., Limit on stably trapped particle fluxes, *J. Geophys. Res.*, 1966, vol. 71, pp. 1–28.
18. Tverskoy, B.A., Stability of the Earth's radiation belts, *Geomagn. Aeron.*, 1967, vol. 7, pp. 226–242.
19. Yakhnina, T.A. and Yakhnin, A.G., Proton precipitation to the equator of the isotropic boundary during the geomagnetic storm on November 20–29, 2003, *Cosmic Research,* 2014, vol. 52, no. 1, pp. 79–85.
20. Zhang, Y., Paxton, L.J., and Zheng, Y., Interplanetary shock induced ring current auroras, *J. Geophys. Res.*, 2008, vol. 113, A01212. doi: 10.1029/2007JA012554
21. Tverskoy, B.A., Mechanism of forming the structure of the ring current of magnetic storms, *Geomagn. Aeron.*, 1997, vol. 37, no. 5, pp. 29–34.
22. Tverskaya, L.V., Boundary of injection of electrons into the Earth's magnetosphere, *Geomagn. Aeron.*, 1986, vol. 26, p. 864.
23. Pavlov, N.N., Tverskaya, L.V., Tverskoy, B.A., and Chuchkov, E.A., Variations of energetic particles of radiation belts during a strong magnetic storm on March 24–26, 1991, *Geomagn. Aeron.*, 1993, vol. 33, no. 6, p. 41.
24. Kalegaev V.V., Vlasova N.A. The Earth's magnetosphere response to interplanetary medium conditions on January 21–22, 2005 and on December 14–15, 2006, *Adv. Space Res.*, 2014, vol. 54, pp. 517-527.

Translated by A. Lidvansky